Progress In Electromagnetics Research C, Vol. 41, 175–188, 2013

A HOMOGENOUS REFERENCE CELLS SELECTOR FOR CFAR DETECTOR IN HIGHLY HETEROGENEOUS ENVIRONMENT

Ling Jiang Kong*, Xin Yi Peng, and Tian Xian Zhang

School of Electronic Engineering, University of Electronic Science and Technology of China, Chengdu, Sichuan, China

Abstract—This paper considers the radar scenes which contain numerous rapidly changing terrains, i.e., there are more than one clutter-edge in the environment. This kind of radar scenes incurs sharply degradation in the performance of the present adaptive constant false alarm rate (CFAR) detectors as the statistical characteristic of reference cells is highly heterogeneous. To solve this problem, we propose a homogenous reference cells selector to improve the performance of CFAR detector in highly heterogeneous environment. The selector is comprised of an M-N clutter-edge detector cascading a terrain classifier. The M-N clutter-edge detector is used to obtain multiple clutter-edges in heterogeneous environment. With the detected clutter-edges, the terrain classifier is derived to obtain identical distributed range cells. Based on the selector, a modified Log-t-CFAR detector is suggested. Finally, the performance of the proposed selector and CFAR detector is evaluated by measured data and computer simulation.

1. INTRODUCTION

Adaptive constant false alarm rate (CFAR) detectors are widely used in radar systems. In these schemes, the CFAR detectors are based on the assumption that the reference cells share the identical statistical characteristic with the cell under test (CUT) [1–7], i.e., the background is homogenous. Unfortunately, in many real-world scenes, the homogeneity assumption is not satisfied any more, e.g., from water to land. This heterogeneous environment incurs rapidly declining in

Received 26 May 2013, Accepted 6 July 2013, Scheduled 9 July 2013

* Corresponding author: Xin Yi Peng (fcadjy@126.com).

the performance of adaptive CFAR detectors, especially when targets are closed to the clutter-edges (i.e., the dividing line of two different distributions).

To solve this problem, several adaptive CFAR detectors in heterogeneous environment have been investigated. In [8, 9], a kind of switching-CFAR has been presented to obtain an optimum detection threshold in homogenous and heterogeneous radar environments. An OS-CFAR detector with binary integration in homogenous and heterogeneous Weibull background has been introduced in [10]. Several clutter-edge detection methods for adaptive CFAR detectors have been, respectively, presented in [11–13]. Nevertheless, the above cited works are barely focus on some simple heterogeneous environments (i.e., there is only one clutter-edge in the environment). Unfortunately, the actual radar scenes, especially with the widely application of the high resolution radars and low grazing angles, always contains a variety of rapidly changing terrains (such as the urban areas and coastal regions), there are more than one clutter-edge in the environment. This kind of highly complicated environment results in significantly degradation in the performance of the above cited CFAR detector. Study of this situation is lacking in current literature, and it is the main topic of this paper.

In this paper we propose a homogenous reference cells selector to choose identical and independent distributed (IID) reference cells with CUT in highly heterogeneous Weibull clutter background. The proposed selector contains an M-N clutter-edge detector cascading a terrain classifier. Specifically, the M-N clutter-edge detector which consists of a sliding clutter-edge locator with an M out of N detection is exploited to detect the locations of multiple clutter-edges. Then according to the detected clutter-edges, range cells not adjacent to each other but with identical distribution are selected by using terrain classifier. Based on the selector, we also propose a modified Log-t-CFAR detector. Thus, the threshold of the proposed CFAR detector can be reasonably calculated by the selected homogenous resolution cells. Finally, the performance advantages of the proposed selector and CFAR detector is verified by the measured data and computer simulation.

The rest of this paper is organized as follows. In Section 2, we describe the homogenous reference cells selector. In Section 3, the homogenous reference cells selector based CFAR detector is introduced. And then the performance of the proposed selector and CFAR detector is verified respectively in 4. Finally, we conclude our discussion.

2. THE HOMOGENOUS REFERENCE CELLS SELECTOR

This section gives the details of the homogenous reference cells selector which contains an M-N clutter-edge detector and a terrain classifier.

2.1. M-N Clutter-edge Detector

Considering a heterogeneous radar scene, the clutter data received from N_L range cells is assumed to be Weibull distribution, whose probability distribution function (pdf) is [14]:

$$f(x,\beta,\lambda) = \frac{\lambda}{\beta} \times \left(\frac{x}{\beta}\right)^{\lambda-1} \exp\left[-(\frac{x}{\beta})^{\lambda}\right], \quad x \geq 0 \tag{1}$$

where β is the scale parameter and λ the shape parameter. N_L range cells are divided into several regions with different clutter parameters by the clutter-edges. We denote the clutter-edge as the dividing-line of two neighboring regions. As shown in Figure 1, the distribution parameters of the clutter in the regions A, B, C and D are different. We also assume that the clutter-edges only exist in the region under test.

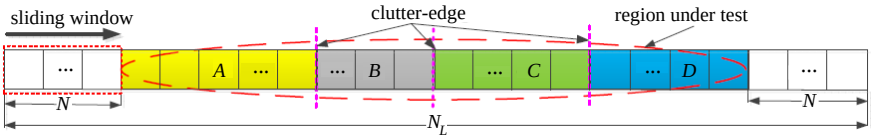

Figure 1. Schematic diagram of received data arrangement.

In order to detect the clutter-edges in the region under test, an M-N clutter-edge detector is proposed. As shown in Figure 2, a sliding window of length N slides a range cell at a time from left to right. At every sliding, we employ a clutter-edge locator to detect the location of a possible clutter-edge.

In the sliding window, we define H_0^K as the hypothesis of not having a clutter-edge between the Kth and $(K+1)$th range cells, while H_1^K denote the hypothesis that a clutter-edge is located between the Kth and $(K+1)$th range cells, where $1 \leq K \leq N-1$. And the clutter-edge locator traverse tests H_1^K against H_0^K. After sliding, all the boundaries of adjacent range cells in the region under test are tested N times. The Kth boundary is indeed the clutter-edge when H_1^K is judged more than $M-1$ times, as shown in Figure 2.

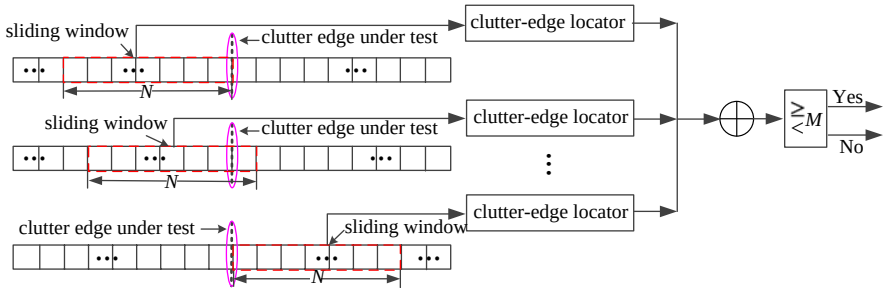

Figure 2. Block diagram of M-N clutter-edge detector.

Next we briefly introduce the clutter-edge locator in the sliding window. Assume that x_i is the ith output sample from an envelop/square law detector and these random samples $\mathbf{x} = [x_1, \ldots, x_N]^T \in R^N$ are independent. And we suppose a clutter-edge is located between the Kth and $(K+1)$th range cells, as shown in Figure 3.

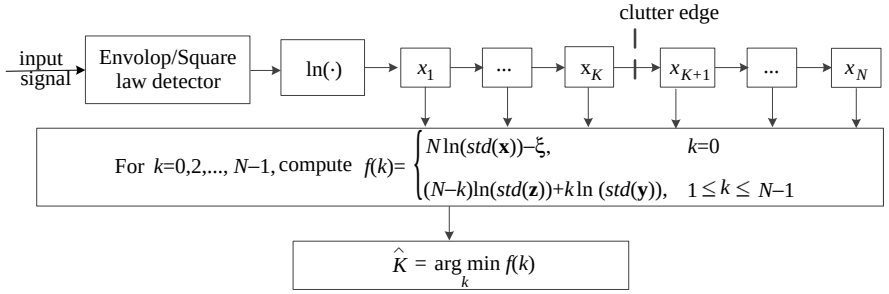

Figure 3. Block of clutter-edge locator.

The clutter-edge partitions $\mathbf{x}$ into $\mathbf{y}_K \in R^K$ and $\mathbf{z}_K \in R^{N-K}$, i.e., $\mathbf{x} = [\mathbf{y}_K, \mathbf{z}_K]^T$, where vector $\mathbf{y}_K$ contains only the first K elements of $\mathbf{x}$, and the joint pdf is $f(\mathbf{y}_K|\vec{a}_y) = \prod_{k=1}^{K} f(y_k|\vec{a}_y)$, therein y_k is the kth element of $\mathbf{y}_K$, and $\vec{a}_y = [\beta_y, \lambda_y]$ are the unknown parameters of $\mathbf{y}_K$ (β_y is the scale parameter and λ_y the shape parameter); $\mathbf{z}_K$ contains the last $N-K$ elements of $\mathbf{x}$, and the joint pdf is $f(\mathbf{z}_K|\vec{a}_z) = \prod_{k=1}^{N-K} f(z_k|\vec{a}_z)$, z_k the kth element of $\mathbf{z}_K$, and $\vec{a}_z = [\beta_z, \lambda_z]$ the unknown parameters of $\mathbf{z}_K$. Specially, $\vec{a}_y$ is different from $\vec{a}_z$.

By H_1^K, the maximum likelihood estimation (MLE) is used to

locate the unknown clutter-edge [13]:

$$(\hat{\vec{a}}_y, \hat{\vec{a}}_z, \hat{K}) \stackrel{\Delta}{=} \arg\max_{K} \left(\sup_{\vec{a}_y} \sum_{k=1}^{K} \ln f(y_k|\vec{a}_y) + \sup_{\vec{a}_z} \sum_{k=1}^{N-K} \ln f(z_k|\vec{a}_z) \right) \quad (2)$$

The maximum likelihood estimation of Weibull distribution parameters are [15]:

$$\begin{cases} \hat{\beta}^{\hat{\lambda}} = \frac{1}{L} \sum\limits_{j=1}^{L} x_j^{\hat{\lambda}} \\ \dfrac{\sum\limits_{j=1}^{L} x_j^{\hat{\lambda}} \ln x_j}{\sum\limits_{j=1}^{L} x_j^{\hat{\lambda}}} - \dfrac{1}{L} \sum\limits_{j=1}^{L} \ln x_j = \dfrac{1}{\hat{\lambda}} \end{cases} \quad (3)$$

where, $\hat{\beta}$ is the estimate of scale parameter and $\hat{\lambda}$ the estimate of shape parameter. Thus, the MLE value of $\vec{a}_y$ and $\vec{a}_z$ are $\hat{\vec{a}}_y = [\hat{\beta}_y, \hat{\lambda}_y]$, $\hat{\vec{a}}_z = [\hat{\beta}_z, \hat{\lambda}_z]$, respectively.

Substitute the MLE value of $\vec{a}_y$ and $\vec{a}_z$ into Equation (2), then:

$$\hat{K} = \arg\min_{1 \le K \le N-1} \left[(N-K) \ln \left(std(\mathbf{z}_K) \right) + K \ln \left(std(\mathbf{y}_K) \right) \right] \quad (4)$$

where $std(\cdot)$ is the expression of the mean square value. With the estimated $\hat{K}$, the minimum description length (MDL) approach is used to test H_0^K against H_1^K [13]:

$$N \ln \left(std(\mathbf{x}) \right) - \left[\left(N - \hat{K} \right) \ln \left(std \left(\mathbf{z}_{\hat{K}} \right) \right) + \hat{K} \ln \left(std \left(\mathbf{y}_{\hat{K}} \right) \right) \right] \underset{H_0^K}{\overset{H_1^K}{\gtrless}} \xi \quad (5)$$

where $\xi = 2 \ln (N)$.

In conclusion, the process of the clutter-edge locator can be illustrated as follows [13],

1. Start with reference data $\mathbf{x} = [x_1, \ldots, x_N]$, with length N, $\xi = 2 \ln(N)$.

2. For $k = 0, 2, \ldots, N-1$, compute:

$$f(k) = \begin{cases} N \ln \left(std \left(\mathbf{x} \right) \right) - \xi, & k = 0 \\ (N-k) \ln \left(std \left(\mathbf{z} \right) \right) + k \ln \left(std \left(\mathbf{y} \right) \right), & 1 \le k \le N-1 \end{cases}$$

where $\mathbf{y} = [y_1, \ldots, y_k]^T$, $\mathbf{z} = [z_{k+1}, \ldots, z_N]^T$.

3. The clutter-edge is located at $\hat{K} = \arg\min_k f(k)$, the clutter-edge doesn't exist if $\hat{K} = 0$.

2.2. Terrain Classifier

The radar surveillance area is usually complicated, such as two kinds of terrains change rapidly and alternately. The M-N clutter-edge detector obtains overmuch clutter-edges, the divided region between adjacent clutter-edges contains finite range cells. This problem would lead to significant performance degradation in adaptive detectors. To solve this problem, we consider two basic principle: 1) the range cells with identical distribution to the CUT are included in the referent window even they are far from the CUT. 2) the range cells with alien distribution to the CUT are excluded in the referent window even they are adjacent to the CUT.

Such as shown in Figure 4, we define that a kind of terrain is equivalent to a pdf, range cells in Terrain $A1$ and $A2$ have identical distribution, while distribution of range cells in Terrain $B1$ and $B2$ is differ from Terrain $A1$ and $A2$. The CUT is located in terrain $A2$. Then, range cells both in Terrain $A1$ and $A2$ can be used as reference cells. In order to identify the distributions between different terrains, the terrain classifier is introduced.

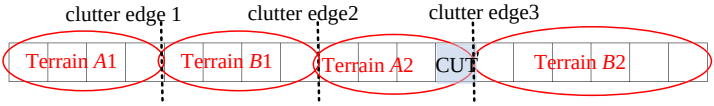

Figure 4. The sketch map of rapidly changed terrain.

As mentioned in Subsection 2.1, the receive data is Weibull distribution whose pdf is totally decided by the scale parameter and shape parameter. By estimating the scale parameter and shape parameter of the regions between adjacent clutter-edges, terrains with identical distribution can be selected. However, the value of the parameters can not be estimated accurately according to finite range cells, it is fluctuating in a range. Thus, we categorize the shape and scale parameters that satisfied a certain range as a kind category. The block diagram of terrain classifier is shown in Figure 5 and the process can be illustrated as:

1. Use Equation (3) to estimate the shape and scale parameters of all the divided regions between adjacent clutter-edges.

2. Sort the estimated shape and scale parameters respectively.

3. According to the range of sorted parameters, divide the shape and scale parameters into T_1 and T_2 parts separately.

4. Number the divided shape and scale parameters from 1 to $F = T_1 \times T_2$, so the receive data has F kinds of terrain.

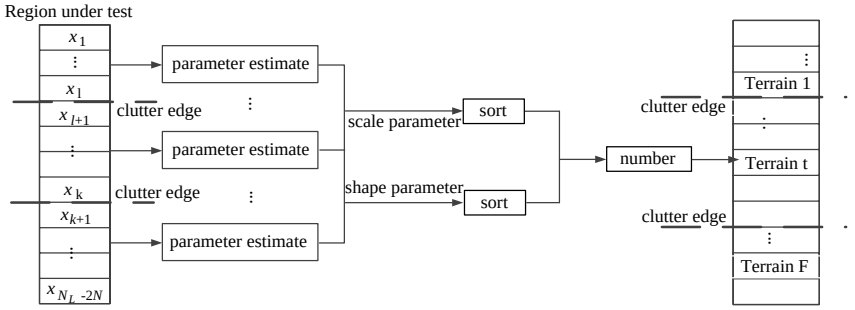

Figure 5. Block diagram of the terrain classifier.

3. THE MODIFIED LOG-T-CFAR DETECTOR

The homogenous reference cells selector is used to determine the reference window of the CUT, in which the range cells are homogenous to the CUT. We set the length of the reference window $L \in (L_{\min}, L_{\max})$. As Figure 1 illustrated, there are $(N_L - 2N)$ range cells in the region under test, in these range cells there are F kinds of terrains and each range cell contains only one kind of terrain which we set as $f_i,\ i = 1, \ldots, N_L - 2N$, while f_{CUT} is set as the kind of terrain within the CUT. We also define $D(i)$ to indicate whether f_{CUT} is equal to f_i, and $D(i)$ can be expressed:

$$D(i) = \begin{cases} 0, & f_i \neq f_{CUT} \\ 1, & f_i = f_{CUT} \end{cases}$$

1. If $\sum_{i=1}^{n} D(i) \geq L_{\max}$, the length of the reference window is $L = L_{\max}$, the reference window contains the nearest $N_{\max}$ range cells that satisfied $D(i) = 1$.

2. Else if, $L_{\min} \leq \sum_{i=1}^{n} D(i) < L_{\max}$, the length of the reference window is $L = \sum_{i=1}^{n} D(i)$, the reference window contains all the $D(i) = 1$ range cells.

3. Else, the length of the reference window is $L = L_{\min}$, the reference window contains all the $D(i) = 1$ range cells and the nearest $L_{\min} - \sum_{i=1}^{n} D(i)$ range cells.

With the decided reference window of CUT, the modified Log-t-

CFAR detector is:

$$\frac{x_{CUT} - \bar{\mathbf{w}}}{std(\mathbf{w})} \underset{H_0}{\overset{H_1}{\gtrless}} T_L \tag{6}$$

where x_{CUT} is the echo of CUT, $\mathbf{w} = [w_1, w_2, \ldots, w_L]$ the range cell samples in the reference window, L the length of $\mathbf{w}$, $\bar{\mathbf{w}}$ the sample mean, T_L the detector threshold which is related to L and satisfies the false alarm probability P_{fa}, and the calculation of T_L is deduced in [16].

4. PERFORMANCE ANALYSIS

4.1. Performance of Homogenous Reference Cells Selector

We use MSTAR Public Data two-dimensional clutter data [17] and IPIX measured data [18] to evaluate the performance of the proposed homogenous reference cells selector.

4.1.1. MSTAR Public Data

MSTAR Public Data is measured data of SAR, the clutter usually comes from grassland, forest, cities and other ground clutter which can be well fit by Weibull distribution [19]. The HB06237 of MSTAR Public Data is considered, it is shown in Figure 6.

As the resolution of MSTAR Public Data is high, we assume $M = 36$, $N = 72$, $F = 6$ with two categories of shape parameters and three categories of scale parameters. The results of M-N clutter-edge detector and the terrain classifier are illustrated in Figure 7(a)

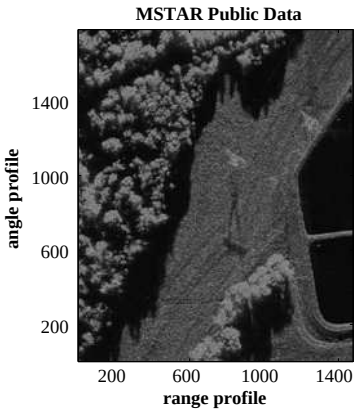

Figure 6. MSTAR public data.

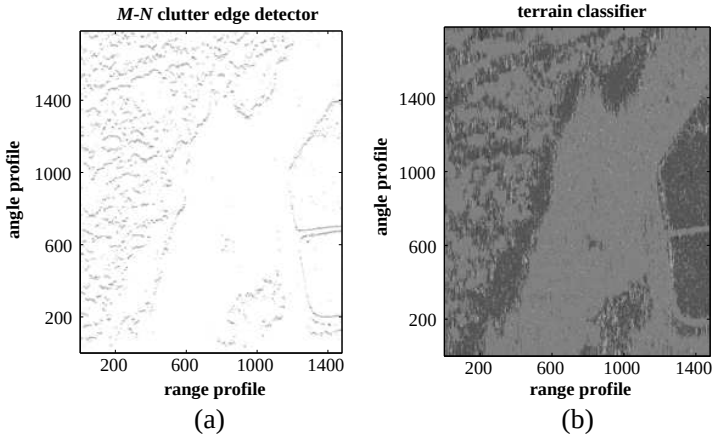

Figure 7. Performance of proposed homogenous reference cells selector of MSTAR public data. (a) Result of M-N clutter-edge detector. (b) Result of the terrain classifier.

and Figure 7(b), respectively. Compare Figure 6 with Figure 7(a), we can see that the clutter-edges are detected accurately by the M-N clutter-edge detector, and from Figure 6, we can see that the terrains in Figure 7(b) are classified validly by the terrain classifier.

4.1.2. IPIX Measured Data

IPIX measured data is collected at the Osborne Head Gunnery Range (OHGR), Dartmouth, Nova Scotia, Canada, with the McMaster University IPIX radar. Specifically, we use the data recorded on November 11, 1993. Radar is located at 44°36.72′N, 63°25.41′W, 100 feet above sea level, the size of the data is 1900×160 [18]. Figure 8 is the IPIX clutter intensity map in the rectangular coordinates system.

Set $M = 16$, $N = 32$, $F = 6$ with three categories of shape parameters and two categories of scale parameters. The results of M-N clutter-edge detector and the terrain classifier are separately shown in Figure 9(a) and Figure 9(b). Comparing Figure 8 and Figure 9(a), the clutter-edges are detected accurately by the M-N clutter-edge detector. And comparing Figure 8 with Figure 9(b), we can see that the terrains are validly classified by the terrain classifier. However, there are a few vertical bars parallel to y-axis at homogeneous areas. Because of the undesirability of radar receiver, the receive data in this area has some outliers data which leads to the parameters misestimating. And the inaccurate parameters further cause the terrain misclassifying in

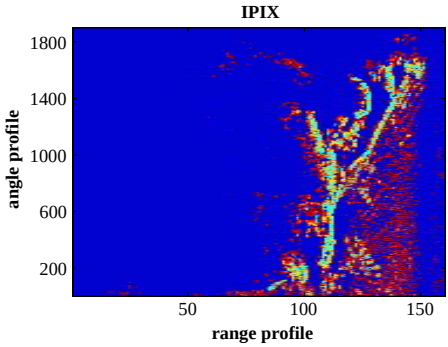

Figure 8. Clutter intensity map of IPIX measured data.

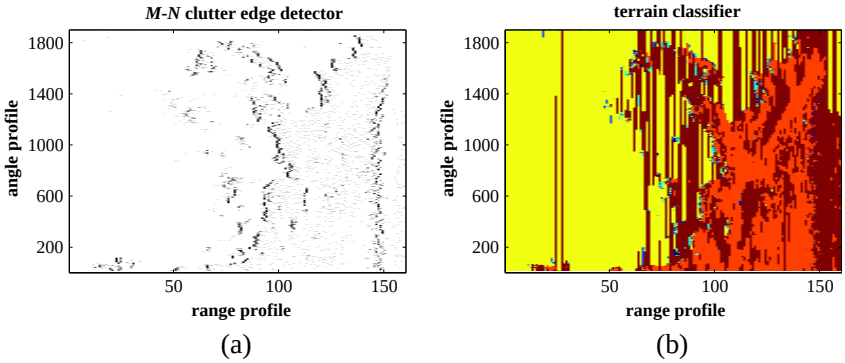

Figure 9. Performance of proposed homogenous reference cells selector of IPIX measured data. (a) Result of M-N clutter-edge detector. (b) Result of the terrain classifier.

this area. And in practical radar application, we can eliminate these vertical bars through the average results of multiple frame data.

4.2. Performance of the Modified Log-t-CFAR Detector

The performance of the proposed CFAR detector is evaluated and compared with the CFAR detector proposed in [13] and traditional Log-t-CFAR detector by computer simulation.

The CFAR detector proposed in [13] is an enhanced Log-t-CFAR detector by incorporating a clutter-edge detection and localization algorithm. And the CFAR detector in [13] is based on the assumption that there is no edge or at most one edge in the reference window.

In this paper, we consider there are 150 range cells with

independent Weibull-distribution random samples. The received signal component is located at the 75th range cell, and follows the Swerling I model with a normalized random Doppler shift uniformly distributed over $(-\pi, \pi]$. Throughout our simulations the probability of false alarm is set to $P_{fa} = 10^{-4}$. The number of Monte-Carlo experiments is 10000. The reference window length of Log-t-CFAR detector and the CFAR detector proposed in [13] is 32, whereas the proposed CFAR detector is $[L_{\min}, L_{\max}] = [8, 32]$.

Figure 11 gives the curves of detection probability versus the signal-to-clutter ratio (SCR) of the proposed CFAR detector, the CFAR detector proposed in [13] and Log-t-CFAR detector in homogenous background and heterogeneous background, the terrain distribution in heterogeneous background is shown in Figure 10. As Figure 11 is illustrated that the proposed CFAR detector performs same as the CFAR detector proposed in [13] and the Log-t-CFAR detector in homogenous environment as all the range cells share the identical statistical characteristic with CUT. While in highly heterogeneous background, the proposed CFAR detector significantly outperforms the CFAR detector proposed in [13] and the Log-t-CFAR detector.

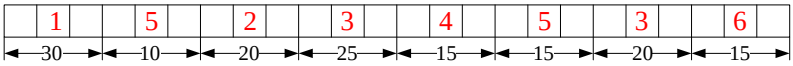

Figure 10. Schematic diagram of terrain location in heterogeneous background of computer simulation.

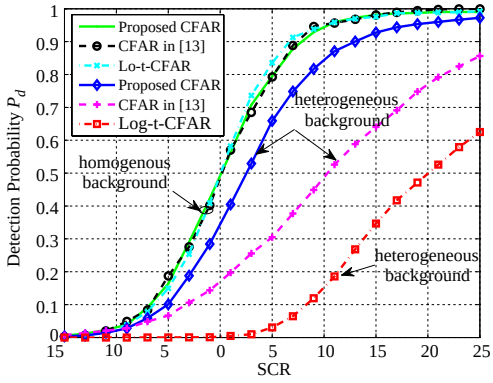

Figure 11. Detection performance of proposed CFAR compared with CFAR proposed in [13] and Log-t-CFAR.

5. CONCLUSION

In this paper, we have proposed a homogenous reference cells selector in highly heterogeneous Weibull clutter background. The selector is composed of an M-N clutter-edge detector concatenating a terrain classifier. The M-N clutter-edge detector is used to obtain multiple clutter-edges in heterogeneous background. With the detected clutter-edges, the IID reference cells in heterogeneous Weibull clutter background are selected by using the terrain classifier. Based on the proposed selector, a modified Log-t-CFAR detector, using resolution cells share identical distribution with CUT as reference window to evaluate threshold, has been proposed. Finally, the effectiveness of the proposed selector is confirmed by measured data, while the performance of the proposed CFAR detector is verified by computer simulation.

The results reveal that the clutter-edges in heterogeneous background can be accurately obtained from the proposed M-N clutter-edge detector and different terrains can be partitioned by the terrain classifier, thus, the proposed selector has good performance in heterogeneous background. And the proposed CFAR detector performs same as the Log-t-CFAR detector and the CFAR detector proposed in [13] in homogenous environment, however, significantly outperforms both the Log-t-CFAR detector and the CFAR detector proposed in [13] in heterogeneous background. Consequently, the proposed CFAR detector has good performance in highly heterogeneous background.

ACKNOWLEDGMENT

This work is sponsored by National Natural Science Foundation of China (61201276), Sichuan Youth Science and Technology Foundation (2011JQ0024), the Fundamental Research Funds for the Central Universities (ZYGX2012Z001 and ZYGX2012YB008) and Program for New Century Excellent Talents in University (A1098524023901001063).

REFERENCES

1. Richards, M. A., *Fundamentals of Statistical Signal Processing*, McGraw-Hill, New York, 2008.
2. Magaz, B., A. Belouchrani, and M. Hamadouche, "Automatic threshold selection in OS-CFAR radar detection using information theoretic criteria," *Progress In Electromagnetics Research B*, Vol. 30, 157–175, 2011.

3. Habib, M. A., M. Barkat, B. Aissa, and T. A. Denidni, "CA-CFAR detection performance of radar targets embedded in 'non centered chi-2 Gamma' clutter," *Progress In Electromagnetics Research*, Vol. 88, 135–148, 2008.
4. Liu, N. N., J. Li, and Y. Cui, "A new detection algorithm based on CFAR for radar image with homogeneous background," *Progress In Electromagnetics Research C*, Vol. 15, 13–22, 2010.
5. Magaz, B., A. Belouchrani, and M. Hamadouche, "A new adaptive linear combined CFAR detector in presence of interfering targets," *Progress In Electromagnetics Research B*, Vol. 34, 367–387, 2011.
6. Hao, C., F. Bandiera, and J. Yang, "Adaptive detection of multiple point-like targets under conic constraints," *Progress In Electromagnetics Research*, Vol. 129, 231–250, 2012.
7. Liu, B. and W. Chang, "A novel range-spread target detection approach for frequency stepped chirp radar," *Progress In Electromagnetics Research*, Vol. 131, 275–292, 2012.
8. Erfanian, S. and V. T. Vakili, "Introducing excision switching-CFAR in K distributed sea clutter," *Signal Processing*, Vol. 89, No. 6, 1023–1031, 2009.
9. Zhang, R. L., W. X. Sheng, and X. F. Ma, "Improved switching CFAR detector for non-homogeneous environments," *Signal Processing*, Vol. 93, No. 1, 35–48, 2013.
10. Hong, S. W. and D. S. Han, "Performance analysis of OS-CFAR with binary integration for Weibull background," *IEEE Transactions on Aerospace and Electronic Systems*, Vol. 49, No. 2, 1357–1366, 2013.
11. Ghobadzadeh, A., A. Pourmottaghi, and M. R. Taban, "Clutter-edge detection and estimation of field parameters in radar detection," *Electrical Engineering (ICEE) Conference*, 1–6, 2011.
12. Chen, B., P. K. Varshney, and J. H. Michels, "Adaptive CFAR detection for clutter-edge heterogeneity using Bayesian inference," *IEEE Transactions on Aerospace and Electronic Systems*, Vol. 39, No. 4, 1462–1470, 2003.
13. Pourmottaghi, A., M. R. Taban, and S. Gazor, "A CFAR detector in a nonhomogenous Weibull clutter," *IEEE Transactions on Aerospace and Electronic Systems*, Vol. 48, No. 2, 1747–1758, 2012.
14. Owolawi, P. A., "Rainfall rate probability density evaluation and mapping for the estimation of rain attenuation in South Africa and surrounding islands," *Progress In Electromagnetics Research*, Vol. 112, 155–181, 2011.

15. Ravid, R., P. K. Varshney, J. H. Michels, "Optimal CFAR detection in Weibull clutter," *IEEE Transactions on Aerospace and Electronic Systems*, Vol. 31, No. 1, 52–64, 1995.
16. Goldstein, G. B., "False-alarm regulation in log-normal and Weibull clutter," *IEEE Transactions on Aerospace and Electronic Systems*, Vol. 9, No. 1, 84–92, 1973.
17. "Moving and stationary target acquisition and recognition (MSTAR)," DARPA/AFRL, Database website: https://www.sdms.afrl.af.mil/datasets/mstar/.
18. Drosopoulos, A., "Description of the OHGR database," Tech. Note No. 94-14, Defence Research Establishment Ottawa, 1994, Database website: http://soma.crl.mcmaster.ca/ipix/dartmouth/index.htm.
19. Skolnik, M. I., *Introduction to Radar Systems*, McGraw-Hill, New York, 2001.